POLITECNICO DI TORINO
Repository ISTITUZIONALE

Radial basis functions-finite differences collocation and a Unified Formulation for bending, vibration and buckling analysis of laminated plates, according to Murakami's zig-zag theory

(Article begins on next page)

19 October 2024

Radial basis functions–finite differences collocation and a Unified Formulation for bending, vibration and buckling analysis of laminated plates, according to Murakami's zig-zag theory

J.D. Rodrigues [a], C.M.C. Roque [a,*], A.J.M. Ferreira [b], E. Carrera [c], M. Cinefra [c]

[a] INEGI, Faculdade de Engenharia, Universidade do Porto, Rua Dr. Roberto Frias, 4200-465 Porto, Portugal
[b] Departamento de Engenharia Mecânica, Faculdade de Engenharia, Universidade do Porto, Rua Dr. Roberto Frias, 4200-465 Porto, Portugal
[c] Department of Aeronautics and Aerospace Engineering, Politecnico di Torino, Corso Duca degli Abruzzi, 24, 10129 Torino, Italy

ABSTRACT

In this paper, we propose to use the Murakami's zig-zag theory for the static and vibration analysis of laminated plates, by local collocation with radial basis functions in a finite differences framework. The equations of motion and the boundary conditions are obtained by the Carrera's Unified Formulation, and further interpolated by a local collocation with radial basis functions and finite differences. This paper considers the analysis of static deformations, free vibrations and buckling loads on laminated composite plates.

1. Introduction

Multilayered structures show a piece-wise continuous displacement field in the thickness plate/shell direction. This change in slope between two adjacent layers, that are considered to be perfectly bonded together, is known as the zig-zag (ZZ) effect, see Fig. 1. The different transverse (both shear and normal components) deformability of the layers is the source of the ZZ effect. Furthermore, these transverse strains are linked with transverse shear and normal stresses that, for equilibrium reasons, are continuous at the each layer interface. These equilibrium conditions are known as interlaminar continuity (IC) for transverse stresses.

There are several possibilities to take into account ZZ and IC in multilayered structures [1–6]. Some of these have been developed in the framework of layer-wise (LW) models, in which the number of the unknown variables depend on the number of layers, but they could result computational expensive, for laminates with large number of layers. Other theories have been formulated in the framework of equivalent single-layer (ESL) models, in which the unknown variables are the same for the whole laminate. The resulting theories are often denoted as zig-zag theories (ZZT). Among the ZZT, three independent approaches are known. These have been denoted in [7] as Lekhnitskii multilayered theory, Ambartsuniam multilayered theory and Reissner multilayered theory. LMT and AMT describe the ZZ effect by enforcing IC via constitutive equations of the layer along with strain-displacement relations. Independent assumptions for displacement and transverse stresses are instead made in the RMT applications.

In the framework of RMT applications, Murakami [8] introduced a function of the thickness coordinate able to emulate the ZZ effect. In [9], such a function was denoted as 'Murakami zig-zag function' (MZZF). MZZF has been used in [8–13] to analyse static response of layered plates and shells in conjunction of RMT applications. Mixed finite elements for plates and shells have been developed in [14–18]. MZZF has been also applied in the framework of plate/shell theories using only displacement variables [13,19]. From implementation point of view, the inclusion of MZZF in existing plate models requires the same efforts that are required by the inclusion of an additional degree of freedom. On the other hand, from numerical point of view, as it will be clear in this paper, inclusion of MZZF leads to significant improvements of the existing plate theories; however, these improvements are difficult to be obtained by the use of other functions which differ by MZZF. An extensive evaluation of the use of MZZF has made in [20,21] using an analytical formulation and in [22] using the finite element method.

In the present work the attention is restricted to the application of ZZF to bending, vibration and buckling analysis of laminated plates by a local collocation scheme with radial basis functions and finite differences. A new displacement theory is used, introducing a quadratic variation of the transverse displacements. This can be seen as a variation of the Murakami's ZZ displacement field [8].

The use of global collocation based on radial basis functions (RBF) has been proposed by Kansa [23] who introduced the concept of solving PDEs by an unsymmetric RBF collocation method based upon the MQ interpolation functions. Unfortunately, this
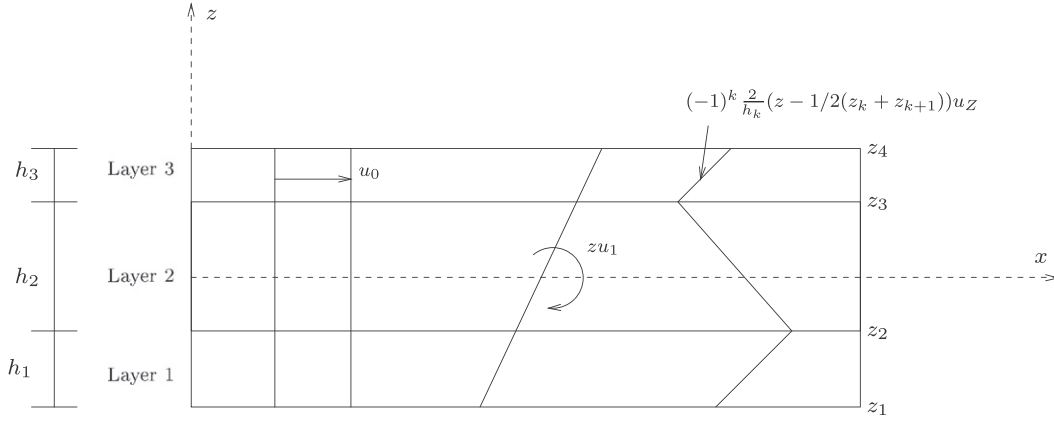
Fig. 1. Scheme of the zig-zag assumptions for a three-layered laminate.

approach produces dense, ill-conditioned, matrices. In order to improve the conditioning number of matrix $\mathbf{A}$, a local collocation approach was formulated by Tolstykh et al. [24], Cecil et al. [25] and Wright and Fornberg [26], in the so-called RBF-FD technique.

The authors have recently applied the global RBF collocation to the static deformations of composite beams and plates [27–29].

In this paper, it is investigated for the first time how the Unified Formulation can be combined with a local radial basis functions–finite differences scheme to the analysis of thick laminated plates, using a variation of the Murakami's zig-zag function, allowing for through-the-thickness deformations. The quality of the present method in predicting static deformations, free vibrations and buckling loads of thin and thick laminated plates is compared and discussed with other methods in some numerical examples.

2. The RBF-FD method

For the sake of completeness, the basic formulation of the RBF-FD method is presented. The finite difference method approximates derivatives of a function $u(x)$ at point $x = x_j$ by:

$$\frac{d^k u(x_j)}{dx^k} \cong \sum_{i=1}^{n} w_{j,i}^k u(x_i) \tag{1}$$

where w^k are weights. In classical finite difference formulas, nodes from i to n are equidistant and weights are computed using polynomial interpolation. This limitation of the spatial distribution of nodes is not desirable for more generic problems. However, using RBFs as an interpolant, a scattered distribution of nodes can be used. Radial basis functions basically depend on the distance between points.

Consider a set of nodes $x_1, x_2, \ldots, x_n \in \Omega \subset \mathbb{R}^n$. The radial basis functions centered at $\mathbf{x}_j$ are defined as

$$\phi(\mathbf{x}) \equiv \phi(\|\mathbf{x} - \mathbf{x}_i\|) \in \mathbb{R}^n, \quad i = 1, \ldots, n \tag{2}$$

where $\|\mathbf{x} - \mathbf{x}_i\|$ is the Euclidian norm. Radial basis functions rely on the euclidean distance between nodes and in some cases on a user-defined shape parameter c.

Although many RBF functions could be used, some of the most used RBFs are [23]:

- Multiquadrics: $\phi(\mathbf{x}) = (\|\mathbf{x} - \mathbf{x}_i\| + c^2)^{\frac{1}{2}}$
- Inverse Multiquadrics: $\phi(\mathbf{x}) = (\|\mathbf{x} - \mathbf{x}_i\| + c^2)^{-\frac{1}{2}}$
- Gaussians: $\phi(\mathbf{x}) = e^{-c^2 \|\mathbf{x} - \mathbf{x}_i\|^2}$
- Thin Plate Splines: $\phi(\mathbf{x}) = \|\mathbf{x} - \mathbf{x}_i\|^2 \log \|\mathbf{x} - \mathbf{x}_i\|$

The approximate solution of a PDE can be represented by a linear combination of smooth radial basis functions, for n grid points

$$u(x) \approx s(x) = \sum_{i=1}^{n} \alpha_i \phi(x - x_i), \quad i = 1, \ldots, N \tag{3}$$

or in matrix-vector notation:

$$\mathbf{u} = \mathbf{A}\alpha \tag{4}$$

where $\mathbf{A} = \phi(x - x_i)$.

Using a global collocation method, we apply a linear operator $\mathscr{L}$ to Eq. (3) to obtain:

$$\mathscr{L}s = \sum_{i=1}^{n} \alpha \mathscr{L}\phi(x - x_i) \tag{5}$$

In this local RBF-FD collocation approach we compute weights p_i such that:

$$\mathscr{L}u(x) = \sum_{i=1}^{n_i} p_i u(x_i) \tag{6}$$

For each node, weights p_i are computed on a subset $\chi_i = [1, \ldots, n_i]$ of the original set of points $\chi = [1, \ldots, n]$ (see Fig. 2).

Subsets χ_i can have an irregular distribution of points and different subsets can have different number of points, increasing the flexibility of the present formulation. In the present paper we usually fix a support distance and consider the nodes within the circle, for each node (also denoted as center).

In order to derive the RBF-FD formulation, an interpolant (3) is considered in a Lagrangean form as

$$s(x) = \sum_{i=1}^{n} \psi_i(x) u(x_i) \tag{7}$$

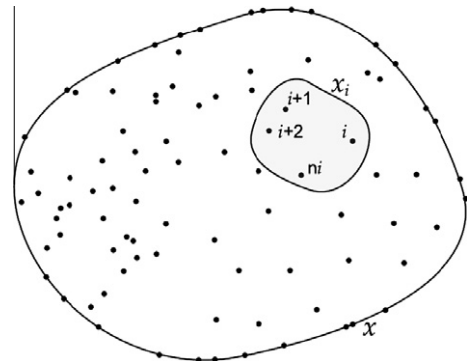where $\psi_i(x_k) = \delta_{ik}$, $k = 1, \ldots, n$.

Fig. 2. Global set χ and local subset χ_i.

A closed form solution exists for the case ($\psi_i(x_k) = \delta_{ik}$), and is given by [30]:

$$\psi_i(x) = \frac{det(A_i(x))}{det(\mathbf{A})} \tag{8}$$

where $A_i(x)$ is obtained by replacing rows i in matrix $\mathbf{A}$ (defined in (4)) by vector

$$\mathbf{B} = [\phi(x - x_1)\phi(x - x_2)\cdots\phi(x - x_n)] \tag{9}$$

The approximation of derivative $\mathcal{L}u(x_j)$ is now performed by applying the linear differential operator on the interpolant in (7) as

$$\mathcal{L}u(x_j) \approx \mathcal{L}s(x_j) = \sum_{i=1}^{n} \mathcal{L}\psi_i(x_j)u(x_i) \tag{10}$$

From (10) and (6) it can be shown that $p_i = \mathcal{L}\psi_i(x_j)$, where such weights are computed by solving the linear system

$$\mathbf{\Phi p} = [\mathcal{L}(\mathbf{B}(x_i))] \tag{11}$$

In (11), $\mathbf{B}(x)$ was computed in Eq. (9), $\mathbf{\Phi}$ is a matrix containing the RBF functions, and $\mathbf{p}$ is a matrix of weights.

For the static and free vibration analysis of plates in bending, a boundary value problem with domain Ω and boundary $\delta\Omega$ is considered. The PDE problem is defined as:

$$\begin{cases} \mathcal{L}\mathbf{u}(x) = \mathcal{H}\ddot{\mathbf{u}}(x) + \mathbf{f}(x), & x \in \Omega \\ \mathcal{D}\mathbf{u}(x) = \mathbf{g}(x), & x \in \delta\Omega \end{cases} \tag{12}$$

Here, $\mathcal{H}$ is a linear differential operator in space, $\ddot{\mathbf{u}}$ represents $\frac{d^2\mathbf{u}}{dt^2}$, and $\mathcal{D}$ is a linear differential operator related to boundary conditions. In the static case, we impose $\mathcal{H}\ddot{\mathbf{u}}(x) = 0$ and we compute weights $\mathbf{p}$ for each node i by solving the linear system of equations

$$\mathbf{\Phi p} = [\mathcal{O}(B(x_i))] \tag{13}$$

where the operator $\mathcal{O}$ is defined by $\mathcal{O} = \mathcal{L}$ in case $i \in \Omega$ or by $\mathcal{O} = \mathcal{D}$ in case $i \in \partial\Omega$.

Solution $\mathbf{u}$ can now be found by assembling the $\mathbf{p}$ weights in global matrix $\mathbf{M}$ and then solving the linear algebraic collocation system:

$$\mathbf{Mu} = \mathbf{F} \tag{14}$$

where $\mathbf{M} = \begin{bmatrix} p^\Omega \\ p^{\delta\Omega} \end{bmatrix}$ is the matrix of weights; $\mathbf{u} = \begin{bmatrix} u^\Omega \\ u^{\delta\Omega} \end{bmatrix}$ is the vector of global unknowns and $\mathbf{F} = \begin{bmatrix} \mathbf{f}(x) \\ \mathbf{g}(x) \end{bmatrix}$ is the vector of external forces. In the case of plates in bending, $\mathbf{f}(x)$ represent applied forces on the domain and $\mathbf{g}(x)$ the (essential and natural) boundary conditions.

Assuming an harmonic solution $\mathbf{u}(x,y,z,t) = \mathbf{U}(x,y,z)e^{i\omega t}$, for the free vibration problem, Eq. (12) is rewritten as:

$$\begin{cases} \mathcal{L}U(x) = -w^2\mathcal{H}U(x), & x \in \Omega \\ \mathcal{D}u(x) = 0; \end{cases} \tag{15}$$

where ω is the frequency of natural vibration. The problem defined in (15) in then computed as generalized eigenproblem:

$$\mathbf{MX} = \omega^2\mathbf{KX} \tag{16}$$

where ω are natural frequencies, and $\mathbf{X}$ are the vectors of modes of vibration. The matrix $\mathbf{M}$ was computed in (14), and matrix $\mathbf{K}$ containing weights $\mathbf{p}$ for each node i is build using Eq. (13) using operators $\mathcal{H}$ and 0, depending on i being a domain or boundary node, respectively.

3. The Murakami's zig-zag function

Let us consider a laminated plate composed of perfectly bonded layers, being z the thickness coordinate of the whole plate while z_k is the layer thickness coordinate. a and h are length and thickness of the square laminated plate, respectively. The adimensional layer coordinate $\zeta_k = (2z_k)/h_k$ is further introduced (h_k is the thickness of the kth layer). The Murakami's zig-zag function $Z(z)$ was defined according to the following formula [8]

$$Z(z) = (-1)^k\zeta_z \tag{17}$$

$Z(z)$ has the following properties:

(1) It is a piece-wise linear function of layer coordinates z_k,
(2) $Z(z)$ has unit amplitude for the whole layers,
(3) the slope $Z'(z) = \frac{dZ}{dz}$ assumes opposite sign between two-adjacent layers. Its amplitude is layer thickness independent.

A possible FSDT theory has been investigated by Carrera [31] and Demasi [32], ignoring the through-the-thickness deformations:

$$u = u_0 + zu_1 + (-1)^k\frac{2}{h_k}\left(z - \frac{1}{2}(z_k + z_{k+1})\right)u_Z \tag{18}$$

$$v = v_0 + zv_1 + (-1)^k\frac{2}{h_k}\left(z - \frac{1}{2}(z_k + z_{k+1})\right)v_Z \tag{19}$$

$$w = w_0 \tag{20}$$

The additional degrees of freedom u_Z, v_z have a meaning of displacement, and its amplitude is layer independent.

A refinement of FSDT by inclusion of ZZ effects and transverse normal strains was introduced in Murakami's original ZZF, defined by the following displacement field:

$$u = u_0 + zu_1 + (-1)^k\frac{2}{h_k}\left(z - \frac{1}{2}(z_k + z_{k+1})\right)u_Z \tag{22}$$

$$v = v_0 + zv_1 + (-1)^k\frac{2}{h_k}\left(z - \frac{1}{2}(z_k + z_{k+1})\right)v_Z \tag{23}$$

$$w = w_0 + zw_1 + z^2w_2 \tag{24}$$

where z_k, z_{k+1} are the bottom and top z-coordinates at each layer. Eq. (24) can be seen as an alternative to the original zig-zag function by Murakami.

4. The Unified Formulation

The Unified Formulation (UF) proposed by Carrera [9,33–35], also known as CUF, is a powerful framework for the analysis of beams, plates and shells. The salient feature of CUF is the unified manner in which all considered variables (displacements and stresses) can be treated. This formulation has been applied in several finite element analysis, either using the Principle of Virtual Displacements, or by using the Reissner's Mixed Variational theorem. The stiffness matrix components, the external force terms or the inertia terms can be obtained directly with this UF, irrespective of the shear deformation theory being considered.

In this section, the fundamental nuclei are obtained by means of the Carrera's Unified Formulation. These allow the derivation of the equations of motion and boundary conditions, in weak form for the finite element analysis; and in strong form for the present RBF collocation.

4.1. Governing equations and boundary conditions in the framework of Unified Formulation

If a multi-layered plate with N_l layers is considered, the Principle of Virtual Displacements (PVD) for the pure-mechanical case reads:

$$\sum_{k=1}^{N_l}\int_{\Omega_k}\int_{A_k}\left\{\delta\epsilon_{pG}^{k}{}^T\sigma_{pC}^k + \delta\epsilon_{nG}^{k}{}^T\sigma_{nC}^k\right\}d\Omega_k\,dz = \sum_{k=1}^{N_l}\delta L_e^k \tag{25}$$

where Ω_k and A_k are the integration domains in plane (x, y) and z direction, respectively. Here, k indicates the layer and T the transpose of a vector, and δL_e^k is the external work for the kth layer. G means geometrical relations and C constitutive equations.

The steps to obtain the governing equations are:

- Substitution of the geometrical relations (subscript G).
- Substitution of the appropriate constitutive equations (subscript C).
- Introduction of the Unified Formulation.

Stresses and strains are separated into in-plane and normal components, denoted respectively by the subscripts p and n. The mechanical strains in the kth layer can be related to the displacement field $\mathbf{u}^k = \{u_x^k, u_y^k, u_z^k\}$ via the geometrical relations:

$$
\begin{aligned}
\boldsymbol{\epsilon}_{pG}^k &= [\epsilon_{xx}, \epsilon_{yy}, \gamma_{xy}]^{kT} = \mathbf{D}_p^k \mathbf{u}^k, \\
\boldsymbol{\epsilon}_{nG}^k &= [\gamma_{xz}, \gamma_{yz}, \epsilon_{zz}]^{kT} = \left(\mathbf{D}_{np}^k + \mathbf{D}_{nz}^k\right) \mathbf{u}^k,
\end{aligned}
\tag{26}
$$

wherein the differential operator arrays are defined as follows:

$$
\mathbf{D}_p^k = \begin{bmatrix} \partial_x & 0 & 0 \\ 0 & \partial_y & 0 \\ \partial_y & \partial_x & 0 \end{bmatrix}, \quad
\mathbf{D}_{np}^k = \begin{bmatrix} 0 & 0 & \partial_x \\ 0 & 0 & \partial_y \\ 0 & 0 & 0 \end{bmatrix}, \quad
\mathbf{D}_{nz}^k = \begin{bmatrix} \partial_z & 0 & 0 \\ 0 & \partial_z & 0 \\ 0 & 0 & \partial_z \end{bmatrix},
\tag{27}
$$

The 3D constitutive equations are given as:

$$
\begin{aligned}
\boldsymbol{\sigma}_{pC}^k &= \mathbf{C}_{pp}^k \boldsymbol{\epsilon}_{pG}^k + \mathbf{C}_{pn}^k \boldsymbol{\epsilon}_{nG}^k \\
\boldsymbol{\sigma}_{nC}^k &= \mathbf{C}_{np}^k \boldsymbol{\epsilon}_{pG}^k + \mathbf{C}_{nn}^k \boldsymbol{\epsilon}_{nG}^k
\end{aligned}
\tag{28}
$$

with

$$
\begin{aligned}
\mathbf{C}_{pp}^k &= \begin{bmatrix} C_{11} & C_{12} & C_{16} \\ C_{12} & C_{22} & C_{26} \\ C_{16} & C_{26} & C_{66} \end{bmatrix}, \quad
\mathbf{C}_{pn}^k = \begin{bmatrix} 0 & 0 & C_{13} \\ 0 & 0 & C_{23} \\ 0 & 0 & C_{36} \end{bmatrix}, \\
\mathbf{C}_{np}^k &= \begin{bmatrix} 0 & 0 & 0 \\ 0 & 0 & 0 \\ C_{13} & C_{23} & C_{36} \end{bmatrix}, \quad
\mathbf{C}_{nn}^k = \begin{bmatrix} C_{55} & C_{45} & 0 \\ C_{45} & C_{44} & 0 \\ 0 & 0 & C_{33} \end{bmatrix}
\end{aligned}
\tag{29}
$$

According to the Unified Formulation by Carrera, the three displacement components u_x, u_y and u_z and their relative variations can be modelled as:

$$
\begin{aligned}
(u_x, u_y, u_z) &= F_\tau(u_{x\tau}, u_{y\tau}, u_{z\tau}), \qquad (\delta u_x, \delta u_y, \delta u_z) \\
&= F_s(\delta u_{xs}, \delta u_{ys}, \delta u_{zs})
\end{aligned}
\tag{30}
$$

where F_τ and F_s can be general functions of the thickness coordinate z. A Taylor expansion from first up to 4th order: $F_0 = z^0 = 1$, $F_1 = z^1 = z, \ldots, F_N = z^N, \ldots, F_4 = z^4$ is taken if an Equivalent Single Layer (ESL) approach is used.

Substituting the geometrical relations, the constitutive equations and the Unified Formulation into the variational statement PVD, for the kth layer, one obtains the governing equations for a multi-layered plate subjected to mechanical loadings:

$$
\delta \mathbf{u}_s^{kT} : \mathbf{K}_{uu}^{k\tau s} \mathbf{u}_\tau^k = \mathbf{P}_{u\tau}^k
\tag{31}
$$

and the corresponding Neumann-type boundary conditions on Γ_k:

$$
\boldsymbol{\Pi}_d^{k\tau s} \mathbf{u}_\tau^k = \boldsymbol{\Pi}_d^{k\tau s} \bar{\mathbf{u}}_\tau^k,
\tag{32}
$$

where $\mathbf{K}_{uu}^{k\tau s}$ and $\boldsymbol{\Pi}_d^{k\tau s}$ are the fundamental nuclei and $\mathbf{P}_{u\tau}^k$ are variationally consistent loads with applied pressure. The explicit forms of the fundamental nuclei are given in Appendix A. For more details about the mathematical passages to obtain the governing equations and boundary conditions one can refer to [36].

4.2. Dynamic governing equations

The PVD for the dynamic case is expressed as:

$$
\sum_{k=1}^{N_l} \int_{\Omega_k} \int_{A_k} \left\{ \delta \boldsymbol{\epsilon}_{pG}^{k\,T} \boldsymbol{\sigma}_{pC}^k + \delta \boldsymbol{\epsilon}_{nG}^{k\,T} \boldsymbol{\sigma}_{nC}^k \right\} d\Omega_k\, dz
$$

$$
= \sum_{k=1}^{N_l} \int_{\Omega_k} \int_{A_k} \rho^k \delta \mathbf{u}^{kT} \ddot{\mathbf{u}}^k d\Omega_k\, dz + \sum_{k=1}^{N_l} \delta L_e^k
\tag{33}
$$

where ρ^k is the mass density of the kth layer and double dots denote acceleration.

By substituting the geometrical relations, the constitutive equations and the Unified Formulation, we obtain the following governing equations:

$$
\delta \mathbf{u}_s^{kT} : \mathbf{K}_{uu}^{k\tau s} \mathbf{u}_\tau^k = \mathbf{M}^{k\tau s} \ddot{\mathbf{u}}_\tau^k + \mathbf{P}_{u\tau}^k
\tag{34}
$$

In the case of free vibrations one has:

$$
\delta \mathbf{u}_s^{kT} : \mathbf{K}_{uu}^{k\tau s} \mathbf{u}_\tau^k = \mathbf{M}^{k\tau s} \ddot{\mathbf{u}}_\tau^k
\tag{35}
$$

where $\mathbf{M}^{k\tau s}$ is the fundamental nucleus for the inertial term. For the explicit expression of $\mathbf{M}^{k\tau s}$, see Appendix A.

The geometrical and mechanical boundary conditions are the same of the static case.

Resorting to the displacement field in Eqs. (22)–(24), we choose vectors $F_t = \begin{bmatrix} 1 & z & (-1)^k \frac{2}{h_k}\left(z - \frac{1}{2}(z_k + z_{k+1})\right) \end{bmatrix}$ for displacements u, v, and $F_t = [1 \quad z \quad z^2]$ for displacement w. We then obtain all terms of the equations of motion by integrating through the thickness direction.

It is interesting to note that under this combination of the Unified Formulation and RBF collocation, the collocation code depends only on the choice of F_t, F_s, in order to solve this type of problems. We designed a MATLAB code that just by changing F_t, F_s can analyse static deformations, free vibrations and buckling loads for any type of C° shear deformation theory. An obvious advantage of the present methodology is that the tedious derivation of the equations of motion and boundary conditions for a particular shear deformation theory is no longer a problem.

5. Numerical examples

A Chebyshev grid and a Wendland function, given by

$$
\phi(r) = (1 - cr)_+^8 (32(cr)^3 + 25(cr)^2 + 8cr + 1)
\tag{36}
$$

is considered in all forthcoming examples. The shape parameter (c) was obtained by an optimization procedure, as detailed in Ferreira and Fasshauer [37]. We consider a plate with side $a = 2$, and a local support distance $d_{max} = 1.5$.

5.1. Static problems-cross-ply laminated plates

A simply supported square laminated plate of side a and thickness h is composed of four equally layers oriented at [0°/90°/90°/0°]. The plate is subjected to a sinusoidal vertical pressure of the form

$$
p_z = P \sin\left(\frac{\pi x}{a}\right) \sin\left(\frac{\pi y}{a}\right)
$$

with the origin of the coordinate system located at the lower left corner on the midplane and P the maximum load (at center of plate).

The orthotropic material properties for each layer are given by

$$
E_1 = 25.0 E_2 \qquad G_{12} = G_{13} = 0.5 E_2 \qquad G_{23} = 0.2 E_2 \qquad \nu_{12} = 0.25
$$

The in-plane displacements, the transverse displacements, the normal stresses and the in-plane and transverse shear stresses are presented in normalized form as

$$\bar{w} = \frac{10^2 w_{(a/2,a/2,0)} h^3 E_2}{Pa^4}, \quad \bar{\sigma}_{xx} = \frac{\sigma_{xx(a/2,a/2,h/2)} h^2}{Pa^2}, \quad \bar{\sigma}_{yy} = \frac{\sigma_{yy(a/2,a/2,h/4)} h^2}{Pa^2},$$

$$\bar{\tau}_{xz} = \frac{\tau_{xz(0,a/2,0)} h}{Pa}, \quad \bar{\tau}_{xy} = \frac{\tau_{xy(0,0,h/2)} h^2}{Pa^2}$$

In Table 1, we present results for the present ZZ theory, using 11×11 up to 21×21 points. We compare results with higher-order solutions by Reddy [38], FSDT solutions by Reddy and Chao [39], and an exact solution by Pagano [40]. Our ZZ theory produces excellent results, when compared with other HSDT theories, for all a/h ratios, for transverse displacements, normal stresses and transverse shear stresses. In Fig. 3, the σ_{xx} evolution across the thickness direction is illustrated, for $a/h = 4$, using 21×21 points. In Fig. 4, the τ_{xz} evolution across the thickness direction is illustrated, for $a/h = 4$, using 21×21 points. Note that the transverse shear stresses are obtained directly from the constitutive equations.

Table 1
[0°/90°/90°/0°] square laminated plate under zig-zag formulation.

$\frac{a}{h}$	Method	$\bar{w}$	$\bar{\sigma}_{xx}$	$\bar{\sigma}_{yy}$	$\bar{\tau}_{zx}$	$\bar{\tau}_{xy}$
4	HSDT [38]	1.8937	0.6651	0.6322	0.2064	0.0440
	FSDT [39]	1.7100	0.4059	0.5765	0.1398	0.0308
	elasticity [40]	1.954	0.720	0.666	0.270	0.0467
	Present (11×11 grid)	1.8928	0.6405	0.8505	0.2160	0.0436
	Present (13×13 grid)	1.8931	0.6408	0.8506	0.2160	0.0436
	Present (17×17 grid)	1.8931	0.6408	0.8506	0.2160	0.0436
	Present (21×21 grid)	1.8931	0.6408	0.8506	0.2160	0.0436
10	HSDT [38]	0.7147	0.5456	0.3888	0.2640	0.0268
	FSDT [39]	0.6628	0.4989	0.3615	0.1667	0.0241
	Elasticity [40]	0.743	0.559	0.403	0.301	0.0276
	Present (11×11 grid)	0.7223	0.5457	0.4196	0.2976	0.0269
	Present (13×13 grid)	0.7227	0.5460	0.4193	0.2979	0.0269
	Present (17×17 grid)	0.7227	0.5460	0.4194	0.2979	0.0269
	Present (21×21 grid)	0.7227	0.5460	0.4194	0.2978	0.0269
100	HSDT [38]	0.4343	0.5387	0.2708	0.2897	0.0213
	FSDT [39]	0.4337	0.5382	0.2705	0.1780	0.0213
	Elasticity [40]	0.4347	0.539	0.271	0.339	0.0214
	Present (11×11 grid)	0.4137	0.5203	0.2643	0.3125	0.0200
	Present (13×13 grid)	0.4349	0.5426	0.2723	0.3393	0.0214
	Present (17×17 grid)	0.4296	0.5366	0.2701	0.3346	0.0211
	Present (21×21 grid)	0.4294	0.5364	0.2699	0.3345	0.0211
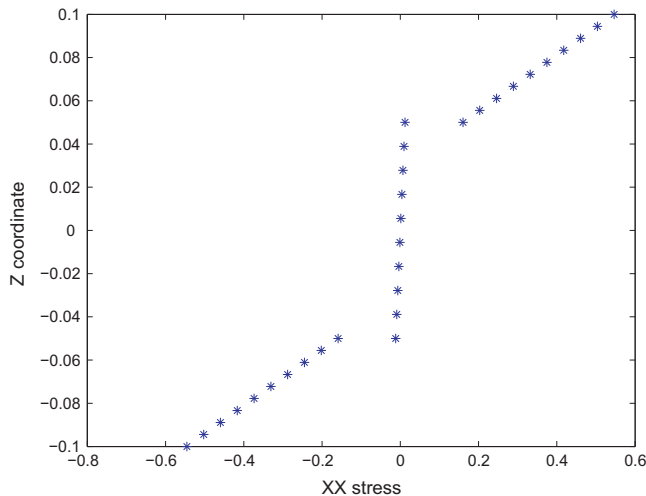
Fig. 3. Normalized normal σ_{xx} stress for $a/h = 10$, 21×21 points.
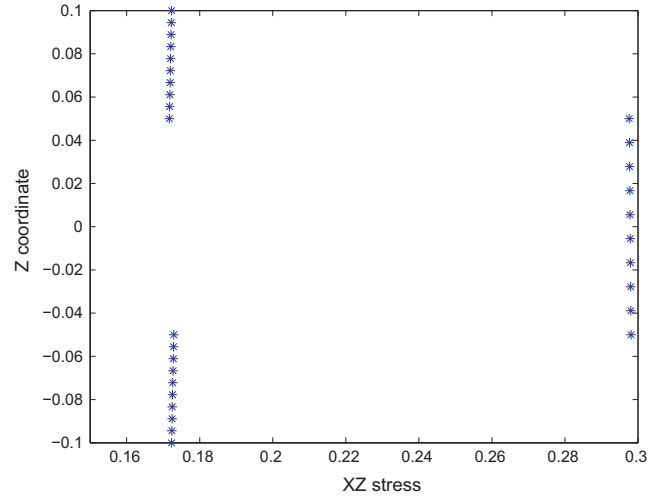

Fig. 4. Normalized transverse τ_{xz} stress for $a/h = 10$, 21×21 points.

5.2. Free vibration problems-cross-ply laminated plates

In this example, all layers of the laminate are assumed to be of the same thickness, density and made of the same linearly elastic composite material. The following material parameters of a layer are used:

$$\frac{E_1}{E_2} = 10, 20, 30 \quad \text{or} \quad 40; \quad G_{12} = G_{13} = 0.6E_2; \quad G_3 = 0.5E_2;$$

$$v_{12} = 0.25$$

The subscripts 1 and 2 denote the directions normal and transverse to the fiber direction in a lamina, which may be oriented at an angle to the plate axes. The ply angle of each layer is measured from the global x-axis to the fiber direction.

The example considered is a simply supported square plate of the cross-ply lamination [0°/90°/90°/0°]. The thickness and length of the plate are denoted by h and a, respectively. The thickness-to-span ratio $h/a = 0.2$ is employed in the computation. Table 2 lists the fundamental frequency of the simply supported laminate made of various modulus ratios of E_1/E_2. It is found that the present meshless results are in very close agreement with the values of Reddy and Khdeir [5,41] and the meshfree results of Liew [42] based on the FSDT.

5.3. Buckling examples

Three-layer [0°/90°/0°] and four-layer [0°/90°/90°0°] square cross-ply laminates are chosen to compute the uni- and bi-axial buckling loads. The plate has width a and thickness h. The span-to-thickness ratio a/h is taken to be 10. All layers are assumed to be of the same thickness and material properties:

Table 2
The normalized fundamental frequency of the simply-supported cross-ply laminated square plate [0°/90°/90°/0°] ($\bar{w} = (wa^2/h)\sqrt{\rho/E_2}$, $h/a = 0.2$).

Method	Grid	E_1/E_2			
		10	20	30	40
Liew [42]		8.2924	9.5613	10.320	10.849
Exact (Reddy, Khdeir) [5,41]		8.2982	9.5671	10.326	10.854
Present ($v_{23} = 0.25$)	13×13	8.4139	9.6627	10.4012	10.9053
	17×17	8.4142	9.6629	10.4013	10.9054
	21×21	8.4142	9.6629	10.4013	10.9054

$E_1/E_2 = 40; G_{12}/E_2 = G_{13}/E_2 = 0.6; G_{23}/E_2 = 0.5; \nu_{12} = 0.25$

Table 3 lists the uni-axial buckling loads of the four-layer simply supported laminated plate. Exact solutions by Khdeir and Librescu [43] and differential quadrature results by Liew et al. [44] based on the FSDT are also presented for comparison. It is found that the critical buckling load is obtained with a few grid points. The present results are in excellent correlation with those of Khdeir and Librescu [43], and those of Liew et al. [44]. Fig. 5 shows the first four buckling modes, for uni-axial buckling load of four-layer [0°/90°/90°/0°] simply supported laminated plate ($\overline{N} = \overline{N}_{xx}a^2/(E_2h^3)$, $\overline{N}_{xy} = 0$, $\overline{N}_{yy} = 0$), using a grid of 13 × 13 points.

Table 4 tabulates the bi-axial buckling loads of the [0°/90°/0°] laminated plate. The laminated plate is simply supported along the edges parallel to the x-axis while the other two edges may be simply supported (S), or clamped (C). The notations SS, SC, and CC refer to the boundary conditions of the two edges parallel to the x-axis only.

In Fig. 6, it is illustrated the first four buckling modes for bi-axial buckling load of three-layer [0°/90°/0°] simply supported lami-

Table 3
Uni-axial buckling load of four-layer [0°/90°/90°/0°] simply supported laminated plate ($\overline{N} = \overline{N}_{xx}a^2/(E_2h^3)$, $\overline{N}_{xy} = 0$, $\overline{N}_{yy} = 0$).

Grid	Present	Liew et al. [44]	Khdeir and Librescu [43]
13 × 13	23.8097	23.463	23.453
17 × 17	23.8110		
21 × 21	23.8110		

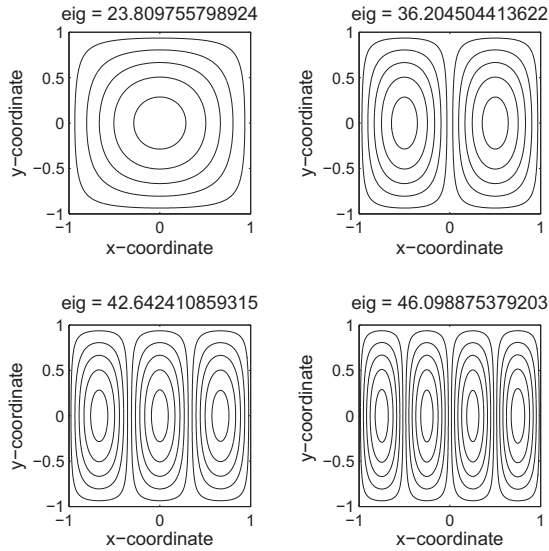**Fig. 5.** First four buckling modes: uni-axial buckling load of four-layer [0°/90°/90°/0°] simply supported laminated plate ($\overline{N} = \overline{N}_{xx}a^2/(E_2h^3)$, $\overline{N}_{xy} = 0$, $\overline{N}_{yy} = 0$), grid 13 × 13 points.

Table 4
Bi-axial buckling load of three-layer [0°/90°/0°] simply supported laminated plate ($\overline{N} = \overline{N}_{xx}a^2/(E_2h^3)$, $\overline{N}_{xy} = 0$, $\overline{N}_{yy} = \overline{N}_{xx}$).

Grid	SS	SC	CC
13 × 13	10.1941	11.7609	13.6646
17 × 17	10.1907	11.7560	13.6631
21 × 21	10.1907	11.7557	13.6629
Liew et al. [44]	10.178	11.575	13.260
Khdeir and Librescu [43]	10.202	11.602	13.290

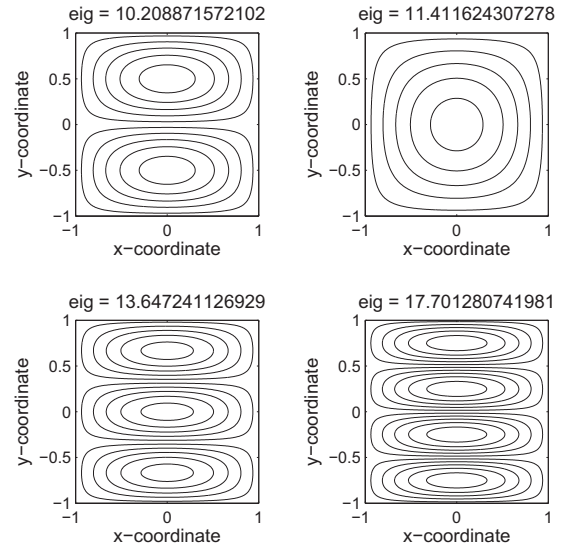**Fig. 6.** First four buckling modes: bi-axial buckling load of three-layer [0°/90°/0°] simply supported (SSSS) laminated plate ($\overline{N} = \overline{N}_{xx}a^2/(E_2h^3)$, $\overline{N}_{xy} = 0$, $\overline{N}_{yy} = \overline{N}_{xx}$), grid 17 × 17 points.

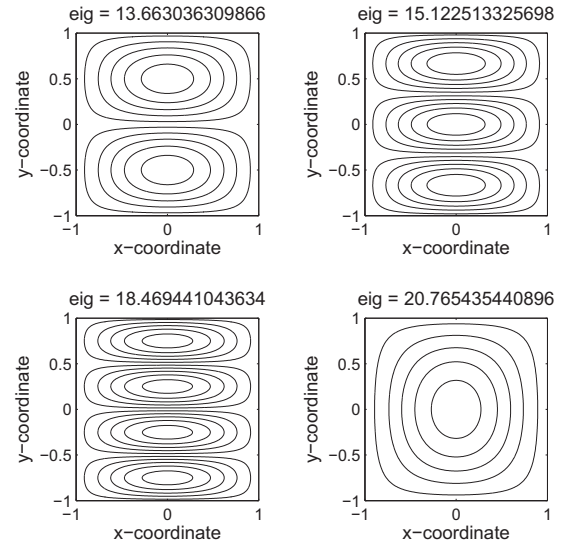**Fig. 7.** First four buckling modes: bi-axial buckling load of three-layer [0°/90°/0°] SCSC laminated plate ($\overline{N} = \overline{N}_{xx}a^2/(E_2h^3)$, $\overline{N}_{xy} = 0$, $\overline{N}_{yy} = \overline{N}_{xx}$), grid 17 × 17 points.

nated plate ($\overline{N} = \overline{N}_{xx}a^2/(E_2h^3)$, $\overline{N}_{xy} = 0$, $\overline{N}_{yy} = \overline{N}_{xx}$), using a grid of 17 × 17 points.

In Fig. 7, it is illustrated the first four buckling modes for bi-axial buckling load of three-layer [0°/90°/0°] SCSC laminated plate ($\overline{N} = \overline{N}_{xx}a^2/(E_2h^3)$, $\overline{N}_{xy} = 0$, $\overline{N}_{yy} = \overline{N}_{xx}$, using a grid of 17 × 17 points.

In Fig. 8, it is illustrated the first four buckling modes for bi-axial buckling load of three-layer [0°/90°/0°] SSSC laminated plate ($\overline{N} = \overline{N}_{xx}a^2/(E_2h^3)$, $\overline{N}_{xy} = 0$, $\overline{N}_{yy} = \overline{N}_{xx}$)), using a grid of 21 × 21 points.

It is found that excellent agreement is achieved for all edge conditions considered when comparing the results obtained by the present local radial basis function–finite differences approach with the FSDT solutions by [43], and those of Liew et al. [44], who use a MLSDQ approach. Note that although comparison with other sources are excellent, the critical loads are related to the second mode (SSSS), fourth mode (SCSC) and third mode (SSSC).
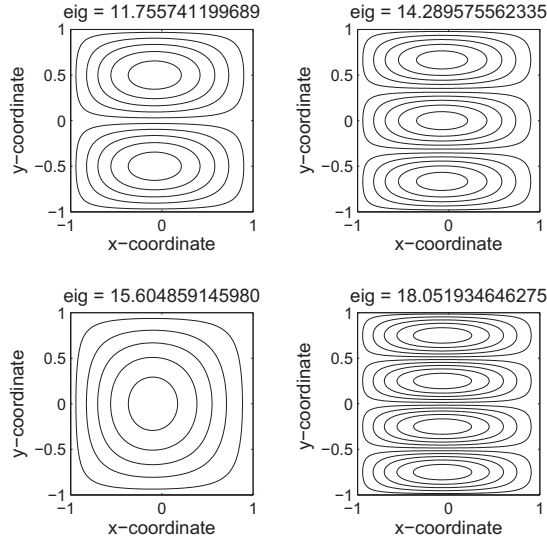
Fig. 8. First four buckling modes: bi-axial buckling load of three-layer $[0°/90°/0°]$ SSSC laminated plate ($\overline{N} = \overline{N}_{xx}a^2/(E_2h^3)$, $\overline{N}_{xy} = 0$, $\overline{N}_{yy} = \overline{N}_{xx}$), grid 21×21 points.

6. Conclusions

In this paper we presented a study using the local radial basis function–finite differences collocation method to analyse static deformations, free vibrations and buckling loads of thin and thick laminated plates using a variation of Murakami's zig-zag function, allowing for through-the-thickness deformations.This has not been done before and fills the gap of knowledge in this research area.

Using the Unified Formulation with the radial basis collocation, all the C^o plate formulations can be easily discretized by radial basis functions–finite differences collocation.

We analysed square cross-ply laminated plates in bending, free vibrations and buckling loads. The present results were compared with existing analytical solutions or competitive finite element solutions and excellent agreement was observed in all cases.

Acknowledgements

Appendix A

The explicit expressions of fundamental nuclei for the equations of motion and boundary conditions, in weak form for the RBF collocation, are listed below:

$$K^{k\tau s}_{uu_{11}} = \left(-\partial^\tau_x\partial^s_xC_{11} - \partial^\tau_y\partial^s_yC_{16} + \partial^\tau_z\partial^s_zC_{55} - \partial^\tau_y\partial^s_xC_{16} - \partial^\tau_y\partial^s_yC_{66}\right)F_\tau F_s$$

$$K^{k\tau s}_{uu_{12}} = \left(-\partial^\tau_x\partial^s_yC_{12} - \partial^\tau_x\partial^s_xC_{16} + \partial^\tau_z\partial^s_zC_{45} - \partial^\tau_y\partial^s_yC_{26} - \partial^\tau_y\partial^s_xC_{66}\right)F_\tau F_s$$

$$K^{k\tau s}_{uu_{13}} = \left(-\partial^\tau_x\partial^s_zC_{13} - \partial^\tau_y\partial^s_zC_{36} + \partial^\tau_z\partial^s_yC_{45} + \partial^\tau_z\partial^s_xC_{55}\right)F_\tau F_s$$

$$K^{k\tau s}_{uu_{21}} = \left(-\partial^\tau_y\partial^s_xC_{12} - \partial^\tau_y\partial^s_yC_{26} + \partial^\tau_z\partial^s_zC_{45} - \partial^\tau_x\partial^s_xC_{16} - \partial^\tau_x\partial^s_yC_{66}\right)F_\tau F_s$$

$$K^{k\tau s}_{uu_{22}} = \left(-\partial^\tau_y\partial^s_yC_{22} - \partial^\tau_y\partial^s_xC_{26} + \partial^\tau_z\partial^s_zC_{44} - \partial^\tau_x\partial^s_yC_{26} - \partial^\tau_x\partial^s_xC_{66}\right)F_\tau F_s$$

$$K^{k\tau s}_{uu_{23}} = \left(-\partial^\tau_y\partial^s_zC_{23} - \partial^\tau_x\partial^s_zC_{36} + \partial^\tau_z\partial^s_yC_{44} + \partial^\tau_z\partial^s_xC_{45}\right)F_\tau F_s$$

$$K^{k\tau s}_{uu_{31}} = \left(\partial^\tau_z\partial^s_xC_{13} + \partial^\tau_z\partial^s_yC_{36} - \partial^\tau_y\partial^s_zC_{45} - \partial^\tau_x\partial^s_zC_{55}\right)F_\tau F_s$$

$$K^{k\tau s}_{uu_{32}} = \left(\partial^\tau_z\partial^s_yC_{23} + \partial^\tau_z\partial^s_xC_{36} - \partial^\tau_y\partial^s_zC_{44} - \partial^\tau_x\partial^s_zC_{45}\right)F_\tau F_s$$

$$K^{k\tau s}_{uu_{33}} = \left(\partial^\tau_z\partial^s_zC_{33} - \partial^\tau_y\partial^s_yC_{44} - \partial^\tau_x\partial^s_yC_{45} - \partial^\tau_y\partial^s_xC_{45} - \partial^\tau_x\partial^s_xC_{55}\right)F_\tau F_s$$

$$(37)$$

$$\Pi^{k\tau s}_{11} = \left(n_x\partial^s_xC_{11} + n_x\partial^s_yC_{16} + n_y\partial^s_xC_{16} + n_y\partial^s_yC_{66}\right)F_\tau F_s$$

$$\Pi^{k\tau s}_{12} = \left(n_x\partial^s_yC_{12} + n_x\partial^s_xC_{16} + n_y\partial^s_yC_{26} + n_y\partial^s_xC_{66}\right)F_\tau F_s$$

$$\Pi^{k\tau s}_{13} = (n_x\partial^s_zC_{13} + n_y\partial^s_zC_{36})F_\tau F_s$$

$$\Pi^{k\tau s}_{21} = \left(n_y\partial^s_xC_{12} + n_y\partial^s_yC_{26} + n_x\partial^s_xC_{16} + n_x\partial^s_yC_{66}\right)F_\tau F_s$$

$$\Pi^{k\tau s}_{22} = \left(n_y\partial^s_yC_{22} + n_y\partial^s_xC_{26} + n_x\partial^s_yC_{26} + n_x\partial^s_xC_{66}\right)F_\tau F_s$$

$$\Pi^{k\tau s}_{23} = (n_y\partial^s_zC_{23} + n_x\partial^s_zC_{36})F_\tau F_s$$

$$\Pi^{k\tau s}_{31} = (n_y\partial^s_zC_{45} + n_x\partial^s_zC_{55})F_\tau F_s$$

$$\Pi^{k\tau s}_{32} = (n_y\partial^s_zC_{44} + n_x\partial^s_zC_{45})F_\tau F_s$$

$$\Pi^{k\tau s}_{33} = \left(n_y\partial^s_yC_{44} + n_y\partial^s_xC_{45} + n_x\partial^s_yC_{45} + n_x\partial^s_xC_{55}\right)F_\tau F_s$$

$$(38)$$

where ∂ indicates the partial derivative and (n_x, n_y) are the components of the normal $\hat{\mathbf{n}}$ to the boundary of domain Ω, along the directions x and y, respectively.

In the dynamic case, the fundamental nucleus for the inertial term $\mathbf{M}^{k\tau s}$ is:

$$M^{k\tau s}_{11} = \rho^kF_\tau F_s; \quad M^{k\tau s}_{12} = 0; \quad M^{k\tau s}_{13} = 0 \qquad (39)$$

$$M^{k\tau s}_{21} = 0; \quad M^{k\tau s}_{22} = \rho^kF_\tau F_s; \quad M^{k\tau s}_{23} = 0 \qquad (40)$$

$$M^{k\tau s}_{31} = 0; \quad M^{k\tau s}_{32} = 0; \quad M^{k\tau s}_{33} = \rho^kF_\tau F_s \qquad (41)$$

References

[1] Lekhnitskii SG. Strength calculation of composite beams. Vestnik inzhen tekhnikov 1935(9).
[2] Lekhnitskii SG. Anisotropic plates. 2nd ed. New York: Gordon and Breach Science Publishers; 1968 [translated from the 2nd Russian ed. by Tsai SW, Cheron, Bordon, Breach].
[3] Ambartsumian SA. Theory of anisotropic shells. Moskwa: Fizmatzig; 1961. NASA TTF-118; 1964 [translated from Russian].
[4] Ambartsumian SA. In: Ashton JE, editor. Theory of anisotropic plates. Stamford: Technomic Publishing Company; 1969 [translated from Russian by Cheron T].
[5] Reddy JN. Mechanics of laminated composite plates, theory and analysis. CRC Press; 1997.
[6] Carrera E. Theories and finite elements for multilayered anisotropic, composite plates and shells. Arch Comput Methods Eng State Art Rev 2002:87–140.
[7] Carrera E. Historical review of zig-zag theories for multilayered plates and shells. Appl Mech Rev 2003(56):287–308.
[8] Murakami H. Laminated composite plate theory with improved in-plane response. J Appl Mech 1986(53):661–6.
[9] Carrera E. Developments, ideas and evaluations based upon the Reissner's mixed theorem in the modeling of multilayered plates and shells. Appl Mech Rev 2001(54):301–29.
[10] Carrera E. Theories and finite elements for multilayered plates and shells: a unified compact formulation with numerical assessment and benchmarking. Arch Comput Methods 2003;10(3).
[11] Toledano A, Murakami H. A high-order laminated plate theory with improved in-plane responses. Int J Solids Struct 1987(23):111–31.
[12] Jing H, Tzeng KG. Refined shear deformation theory of laminated shells. Am Inst Aeronaut Astronaut J 1993(31):765–73.
[13] Carrera E. A study of transverse normal stress effects on vibration of multilayered plates and shells. J Sound Vib 1999(225):803–29.
[14] Rao KM, Meyer-Piening HR. Analysis of thick laminated anisotropic composites plates by the finite element method. Compos Struct 1990:185–213.
[15] Brank B, Carrera E. Multilayered shell finite element with interlaminar continuous shear stresses: a refinement of the Reissner–Mindlin formulation. Int J Numer Methods Eng 2000(48):843–74.
[16] Carrera E, Parisch H. Evaluation of geometrical nonlinear effects of thin and moderately thick multilayered composite shells. Compos Struct 1998:11–24.
[17] Auricchio F, Sacco E. Refined first-order shear deformation theory models for composite laminates. J Appl Mech 2003(70):381–90.
[18] Carrera E, Demasi L. Multilayered finite plate element based on Reissner mixed variational theorem, part I: theory and part II: numerical analysis. Int J Numer Methods Eng 2002(55):191–231.
[19] Bhaskar K, Varadan TK. A higher-order theory for bending analysis of laminated shells of revolution. Comput Struct 1991(40):815–9.
[20] Carrera E. On the use of Murakami's zig-zag function in the modeling of layered plates and shells. Comput Struct 2004(82):541–54.
[21] Brischetto S, Carrera E, Demasi L. Improved bending analysis of sandwich plate by using zig-zag function. Compos Struct 2009;89:408–15.

[22] Demasi L. Refined multilayered plate elements based on Murakami zig-zag functions. Compos Struct 2005;70:308–16.

[23] Kansa EJ. Multiquadrics – a scattered data approximation scheme with applications to computational fluid dynamics. I: surface approximations and partial derivative estimates. Comput Math Appl 1990;19(8/9):127–45.

[24] Tolstykh AI, Lipavskii MV, Shirobokov DA. High-accuracy discretization methods for solid mechanics. Arch Mech 2003;55(5–6):531–53.

[25] Cecil T, Qian J, Osher S. Numerical methods for high dimensional Hamilton–Jacobi equations using radial basis functions. J Comput Phys 2004;196(1):327–47.

[26] Wright GB, Fornberg B. Scattered node compact finite difference-type formulas generated from radial basis functions. J Comput Phys 2006;212(1):99–123.

[27] Ferreira AJM. A formulation of the multiquadric radial basis function method for the analysis of laminated composite plates. Compos Struct 2003;59:385–92.

[28] Ferreira AJM. Thick composite beam analysis using a global meshless approximation based on radial basis functions. Mech Adv Mater Struct 2003;10:271–84.

[29] Ferreira AJM, Roque CMC, Martins PALS. Analysis of composite plates using higher-order shear deformation theory and a finite point formulation based on the multiquadric radial basis function method. Composites: Part B 2003;34:627–36.

[30] Fornberg B, Wright G, Larsson E. Some observations regarding interpolants in the limit of flat radial basis functions. Comput Math Appl 2004;47:37–55.

[31] Carrera E. The use of Murakami's zig-zag function in the modeling of layered plates and shells. Compos Struct 2004;82:541–54.

[32] Demasi L. ∞^3 hierarchy plate theories for thick and thin composite plates: the generalized unified formulation. Compos Struct 2008;84:256–70.

[33] Carrera E. C^0 Reissner–Mindlin multilayered plate elements including zig-zag and interlaminar stress continuity. Int J Numer Methods Eng 1996;39:1797–820.

[34] Carrera E, Kroplin B. Zig-zag and interlaminar equilibria effects in large deflection and post-buckling analysis of multilayered plates. Mech Compos Mater Struct 1997;4:69–94.

[35] Carrera E. Evaluation of layer-wise mixed theories for laminated plate analysis. AIAA J 1998(36):830–9.

[36] Ferreira AJM, Roque CC, Carrera E, Cinefra M. Analysis of thick isotropic and cross-ply laminated plates by radial basis functions and unified formulation. J Sound Vib 2011(330):771–87.

[37] Ferreira AJM, Fasshauer GE. Computation of natural frequencies of shear deformable beams and plates by a RBF-pseudospectral method. Comput Methods Appl Mech Eng 2006;196:134–46.

[38] Reddy JN. A simple higher-order theory for laminated composite plates. J Appl Mech 1984;51:745–52.

[39] Reddy JN, Chao WC. A comparison of closed-form and finite-element solutions of thick laminated anisotropic rectangular plates. Nuclear Eng Des 1981;64:153–67.

[40] Pagano NJ. Exact solutions for rectangular bidirectional composites and sandwich plates. J Compos Mater 1970;4:20–34.

[41] Khdeir AA, Librescu L. Analysis of symmetric cross-ply elastic plates using a higher-order theory, part II: buckling and free vibration. Compos Struct 1988;9:259–77.

[42] Liew KM, Huang YQ, Reddy JN. Vibration analysis of symmetrically laminated plates based on FSDT using the moving least squares differential quadrature method. Comput Methods Appl Mech Eng 2003;192:2203–22.

[43] Khdeir AA, Librescu L. Analysis of symmetric cross-ply elastic plates using a higher-order theory. Part II: buckling and free vibration. Compos Struct 1988;9:259–77.

[44] Liew KM, Huang YQ. Bending and buckling of thick symmetric rectangular laminates using the moving least-squares differential quadrature method. Int J Mech Sci 2003;45:95–114.